

Subcutaneous blood pressure monitoring with an implantable optical sensor

Michael Theodor · Dominic Ruh · Jens Fiala ·
Katharina Förster · Claudia Heilmann · Yiannos Manoli ·
Friedhelm Beyersdorf · Hans Zappe · Andreas Seifert

Published online: 9 May 2013
© Springer Science+Business Media New York 2013

Abstract We introduce a minimally invasive, implantable system that uses pulse transit time to determine blood pressure. In contrast to previous approaches, the pulse wave is detected by a photoplethysmographic (PPG) signal, acquired with high quality directly on subcutaneous muscle tissue. Electrocardiograms (ECG) were measured with flexible, implantable electrodes on the same tissue. PPG detection is realized by a flat 20 mm x 6 mm optoelectronic pulse oximeter working in reflection mode. The optical sensor as well as the ECG electrodes can be implanted using minimally invasive techniques, with only a small incision into the skin, making long-term monitoring of blood pressure in day-to-day life for high-risk patients possible. The *in vivo* measurements presented here show that the deviation to intra-arterial reference measurements of the systolic blood pressure in a physiologically relevant range is only 5.5 mmHg, demonstrated for more than 12 000 pulses. This makes the presented sensor a grade B blood pressure monitor.

Keywords Pulse transit time · Photoplethysmography · Blood pressure monitoring · Medical implant · Optical sensor · Minimally invasive

1 Introduction

Over one billion people worldwide suffer from hypertension. Reliable blood pressure (BP) management is the key to avoid cardiac events resulting from this hypertension. The regular measurement of blood pressure, outside the clinical environment, can optimize necessary drug treatment (O'Brien et al. 2003). Furthermore, continuous monitoring of the pressure can immediately detect a hypertension emergency, which can be life threatening if not treated within one hour (Richard and Irwin 2009).

Blood pressure management can be performed in a manner similar to that employed for diabetes mellitus: the patient adjusts the medication dose based on the results of a blood pressure measurement. An alternative future possibility is that of a closed loop system, consisting of a blood pressure sensor and a drug pump, which regulates the blood pressure level automatically. An implantable drug delivery system for osteoporosis patients has already been tested successfully (Farra et al. 2012).

The problem with these approaches is the current lack of a blood pressure monitoring device that may be used by a mobile patient undertaking the activities of everyday life. The sensor proposed here may serve to fill this gap.

The standard methods presently used to measure blood pressure are predominantly intra-arterial catheters and cuff-based oscillometric monitors. In the case of catheters, distal vessel occlusion, hemorrhage, and infection represent the fundamental complications. In the case of cuff-based monitors, distal limb ischemia and venous stasis – due to frequent

M. Theodor is holder of a Fritz-Hüttinger Scholarship.

M. Theodor (✉) · J. Fiala · D. Ruh · Y. Manoli · H. Zappe ·
A. Seifert
Department of Microsystems Engineering, University of Freiburg,
Georges-Koehler-Allee 102, 79110 Freiburg, Germany
e-mail: michael.theodor@imtek.de

K. Förster · C. Heilmann · F. Beyersdorf
Department of Cardiovascular Surgery,
University Medical Center, Hugstetter Str. 55,
79106 Freiburg, Germany

Y. Manoli
HSG-IMIT, Institute of Micromachining and
Information Technology, Wilhelm-Schickard-Strasse 10,
78052 Villingen-Schwenningen, Germany

inflation or deflation failure – are the most significant drawbacks (Richard and Irwin 2009). As a result, both methods have proved to be impractical for long-term monitoring.

The approach for determining blood pressure presented here is based on pulse transit time (PTT), a quantity closely correlated to blood pressure (Nye 1964). The PTT can be measured extravascularly and without need of a cuff, and thus overcomes the disadvantages of traditional systems.

Several devices for measurement of PTT have been presented, using for example ECG (electrocardiography) and an arm cuff (Ahmad et al. 2012; Asada et al. 2003), or ECG and a pulse oximeter on the finger (Chua and Heneghan 2006; Fung et al. 2004; Lee et al. 2003), two pulse oximeters on one arm (Deb et al. 2007), and even an implantable solution, using ECG and a pulse oximeter mounted directly on an artery (Fiala et al. 2012). Another approach, employing subcutaneously measured photoplethysmographic signals, has already been used to estimate blood pressure based on the amplitude of the signal (Turcott and Pavek 2008).

In this paper, we present a system that uses pulse transit time, the time difference between the R-peak of the ECG and the systolic slope of the photoplethysmogram (PPG), to determine systolic blood pressure. In contrast to previous approaches, the PPG signal is acquired directly from subcutaneous muscle tissue using a minimally invasively implantable sensor. This implant realization provides mobility for the patient without the risk of a misplacement of the sensor, which is critical for extracorporeal devices. The theoretical background on which this method to measure arterial blood pressure is based is presented in the following section. The sensor structure is presented in Section 3. In Section 4, *in vivo* experiments are used to evaluate the sensor characteristics when applied to subcutaneous tissue, and substantiate the stability of the method for long-term systolic blood pressure measurement over a wide physiologically-relevant pressure range.

2 Theory

2.1 Pulse waves

After each heart contraction, the pressure in the aorta rises, and traveling pulse waves pass through the subsequent arterial tree. The most important characteristics of blood pulse waves are their frequency, amplitude, shape and velocity.

A typical pulse waveform is schematically shown in Fig. 1. It is characterized by the steep systolic slope, due to the heart contraction, and the slower decrease that exhibits one or more augmentations formed by reflected waves from other parts of the arterial tree (Millasseau et al. 2006). In particular, the first systolic reflection, known as the augmentation point, has been used as an indicator for arterial

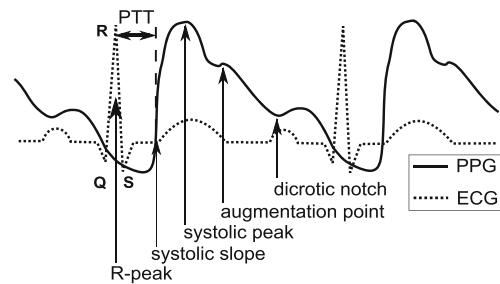


Fig. 1 Schematic representations of a characteristic photoplethysmogram (PPG) and an electrocardiogram (ECG) with characteristic QRS complex. The time between the main peak in the ECG-signal and the steepest part of the systolic slope is the pulse transit time (PTT)

blood pressure and stiffness. The dicotic notch at the end of the systole is caused by the so-called Windkessel-effect in the aorta and provides information on the condition of this blood vessel.

2.2 Photoplethysmography

A photoplethysmogram (PPG) is the arterial blood pulse curve recorded by an optical detector. Standard pulse oximeters employ this measurement method, using two wavelengths for the determination of arterial blood oxygen saturation. When measured with a high signal quality, photoplethysmography is a suitable approach for pulse contour analysis. Whereas the amplitude of the PPG signal changes with tissue perfusion, the shape of the pulse wave remains constant (Millasseau et al. 2006). Thus the PPG signal includes the shape and frequency of the blood pulse and hence the information about the arterial pulse wave.

The sensor presented here measures the PPG directly on subcutaneous muscle tissue. It is designed in a similar fashion to a reflection mode pulse oximeter, with a light source and a detector, separated by an optical barrier, on the same side of the perfused tissue.

2.3 Pulse transit time

Pulse transit time generally describes the time between blood ejection from the heart and the arrival of the travelling pulse wave at a specific measurement point.

The most widespread detection method uses the combination of ECG with a PPG sensor. The dominant R-peak in the ECG is the moment of the heart excitation which leads to blood ejection after a pre-ejection period.

The approach we employ here defines the time between the R-peak and the steepest part of the systolic slope of the PPG as the PTT, as shown in Fig. 1.¹ PTT equals the ratio of travelled path-length s and pulse wave velocity (PWV).

¹This time difference is sometimes also referred to as the pulse arrival time (PAT).

The *PWV* is recognized as a reproducible indicator for cardiovascular risks (Wilkinson et al. 1998) (Blacher et al. 1999), and is well-described by the Moens-Korteweg equation (Fung 2010),

$$PWV = \sqrt{\frac{E \cdot h}{2\rho \cdot a_i}}, \tag{1}$$

where a_i is the inner diameter of the blood vessel; ρ the fluid (blood) density; E the Young’s modulus of the blood vessel wall; and h the thickness of the vessel wall. This relationship describes the *PWV* in a generic blood vessel, neglecting effects of viscosity and thick or inhomogeneous blood vessel walls.

2.4 Blood pressure

Numerous measurements have shown that the Young’s modulus $E(BP)$ of large arteries increases almost linearly with blood pressure within the physiologically relevant pressure range (Bergel 1961). Thus, in this first order approximation, we can write

$$E(BP) = m_E \cdot BP + E_0, \tag{2}$$

where the coefficients m_E and E_0 are patient-specific fit parameters. The Moens-Korteweg Equation may then be written as

$$PWV = \sqrt{\frac{m_E \cdot h}{2\rho \cdot a_i} \cdot BP + \frac{E_0 \cdot h}{2\rho \cdot a_i}}, \tag{3}$$

yielding the following expression for the blood pressure:

$$BP = \frac{2\rho \cdot a_i}{m_E \cdot h} \left(PWV^2 - \frac{E_0 \cdot h}{2\rho \cdot a_i} \right) = \frac{2\rho \cdot a_i}{m_E \cdot h} PWV^2 - \frac{E_0}{m_E}. \tag{4}$$

Recalling that $PTT = \frac{s}{PWV}$, this last expression can be modified to yield

$$BP = \frac{2\rho \cdot a_i \cdot s^2}{m_E \cdot h} \cdot \frac{1}{PTT^2} - \frac{E_0}{m_E}, \tag{5}$$

for constant arterial path length s . Assuming that the density ρ and ratio a_i/h are also constant, we may finally simplify this relationship to take the form

$$BP = m \cdot \frac{1}{PTT^2} + c. \tag{6}$$

The slope m and offset c are again individual fit parameters, which vary from subject to subject, and need to be determined for each patient.

2.5 Calibration and accuracy

Blood pressure determination by pulse transit time has to be calibrated for each individual. The precision of the sensor is an intrinsic parameter which should be measured in advance, before the calibration takes place. For determination of the precision, Gaussian statistics are assumed and the standard deviation of a single measurement σ_{single} was determined by performing a large number of successive measurements.

For optimizing the system accuracy, the calibration procedure should take place over as long a time period practicable. Blood pressure monitoring over 24 h with at least 50 reference points is recommended to enhance the accuracy. The absolute accuracy will then be in the order of the precision σ_{single} .

Relating the PTT-based blood pressure values with the reference blood pressure values yields a linear function,

$$BP_{ref} = m_c BP_{PTT} + c_c, \tag{7}$$

with slope m_c around 1 and offset c_c around 0, where the accuracy of the individual absolute values are strongly influenced by the precision of a single measurement. The simplest calibration procedure is done by taking only two reference points. The corresponding uncertainty can be reduced by separating the two pressure levels as far as possible. Figure 2 shows how a worst case estimate of

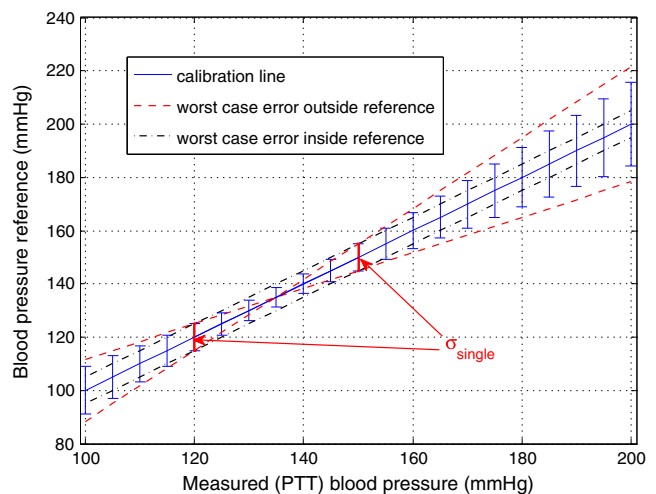


Fig. 2 Accuracy of blood pressure calibration by taking two reference points. In the example, the reference is taken at 120 and 150 mmHg with an uncertainty (precision) of $\sigma_{single} = \pm 5$ mmHg. The blue error bars are the result of the error propagation when each PTT-based pressure level is determined with an uncertainty of σ_{single} . The red dashed lines, connecting lowest and highest levels of the error bars at the reference points, respectively, give a worst case estimate of the accuracy outside the reference points. The black dashdotted lines connect upper with upper and lower with lower level at the reference error bars. These lines include the worst case estimate of the accuracy between the reference points

the accuracy of the system can be determined graphically, dependent on the precision σ_{single} at two given reference points.

Given two reference points ($BP_{PTT1}|BP_{\text{ref1}}$) and ($BP_{PTT2}|BP_{\text{ref2}}$), the accuracy over the complete physiological range can be calculated by Gaussian error propagation, thereby varying the PTT-based values BP_{PTT1} and BP_{PTT2} by σ_{single} . Slope m_c and offset c_c are given by

$$m_c = \frac{BP_{\text{ref2}} - BP_{\text{ref1}}}{BP_{PTT2} - BP_{PTT1}},$$

$$c_c = \frac{BP_{PTT2}BP_{\text{ref1}} - BP_{PTT1}BP_{\text{ref2}}}{BP_{PTT2} - BP_{PTT1}}. \quad (8)$$

The analytical description of the absolute error of the blood pressure – this is the system’s accuracy – can be calculated straightforwardly, but the result is complicated. To better illustrate the error, we show in Fig. 3 four different curves describing the accuracy in the range of 100 – 200 mmHg for four different calibration pairs. The accuracy is given in terms of the precision σ_{single} . Figures 2 and 3 show that the accuracy equals the precision at the reference points, decreases in between these two, and increases for larger or smaller values. Since we assume a constant precision σ_{single} for all blood pressure levels BP_{PTT} , the precision of the calibrated actual pressure values is $m_c\sigma_{\text{single}}$.

Table 1 shows some examples of the averaged uncertainty over the range of 100 – 200 mmHg dependent on the standard deviation σ_{single} of the single PTT-based blood pressure measurement.

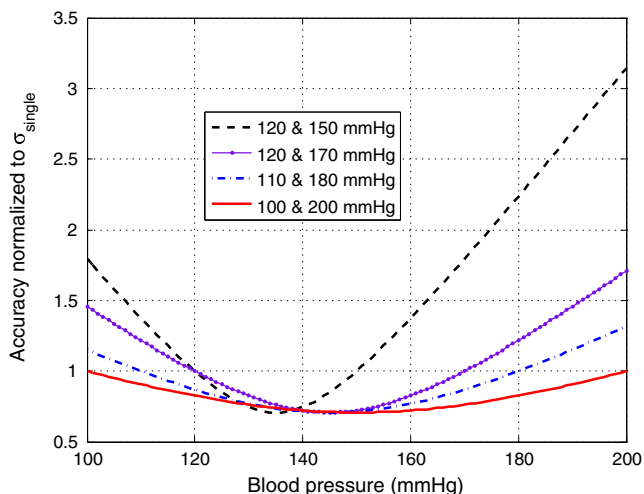


Fig. 3 Absolute accuracy of the PTT-based blood pressure values for a two-point calibration. The calibration values are given in the legend. The accuracy is normalized with respect to σ_{single}

Table 1 Mean absolute error between 100 and 200 mmHg caused by calibration at two reference points which are determined with a precision of σ_{single}

Low calibration point (mmHg)	High calibration point (mmHg)	Mean error in terms of σ_{single}
100 mmHg	200	0.81
110 mmHg	180	0.91
100 mmHg	170	0.94
120 mmHg	170	1.06
100 mmHg	150	1.21
120 mmHg	150	1.55
120 mmHg	140	2.26

3 System design

3.1 Sensor layout

The sensor used for the PTT measurements is a reflection mode pulse oximeter (Moyle 2002). Figure 4 shows the sensor front, which consists of two pairs of photo diodes and LEDs: red at 660 nm and infrared at 935 nm. To prevent interference with the other LED or ambient light of other wavelengths, narrowband photo diodes are employed. The transmitter and receiver for infrared and red light are separated by 10 mm and 7 mm, respectively. The sensor is designed to be capable of measuring blood oxygen saturation; however, for the determination of PTT, one LED and one photo diode would be sufficient.

The back of the sensor includes a dual transimpedance amplifier. This setup minimizes electrical interference between the weak sensor signal and the amplifier, due to the proximity of detector and amplifier. An operational amplifier (Texas Instruments, OPA381) with very low noise is used, with two anti-aliasing filter stages to allow 40 dB/decade suppression of signals higher than the cut-off frequency of 250 Hz.

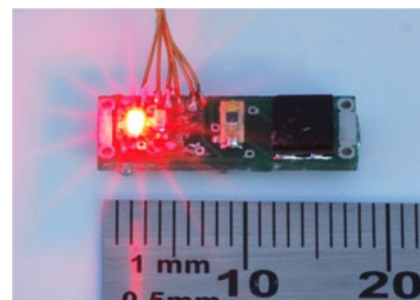


Fig. 4 Front side of the implantable pulse oximeter sensor, showing two photo diodes and two LEDs emitting at 660 nm and 935 nm; picture taken before silicone encapsulation. Two transimpedance amplifiers are mounted on the back of the sensor

Table 2 Amplitudes of the R-peaks of the ECG measurements on subcutaneous tissue for different electrode sizes and various spacings

Electrode spacing	1 cm	3 cm	8 cm
1 cm ² area		0.5 mV	1.1 mV
4 cm ² area	7.2 mV	12.3 mV	23.9 mV
9 cm ² area		15.7 mV	23.5 mV

Driving the LED with high current or using several LEDs in series increases the optical power and hence the sensor signal, but results in a higher power consumption and the risk of tissue warming. As a trade-off, one LED per wavelength was used and driven with a current of 30 mA, which did not cause tissue warming of more than 2 K during evaluation.

For the detection of motion artifacts on an awake subject, an accelerometer might also be included in the system.

3.2 Packaging

The pulse oximeter is coated by a 10 μm Parylene C layer for protection against moisture. Parylene C has been used as an encapsulation material for cardiac pacemakers for several decades (Stieglitz et al. 2002). To avoid damage of the parylene layer and to provide a soft package, the implant is subsequently encapsulated in 0.5 mm thick transparent, biocompatible silicone (MED-1000, NuSil). Med-1000 is certified for use in humans for up to 29 days. The dimensions of the final module used for the measurements are 18 mm x 6 mm at a thickness of 2 mm.

The materials used for the electronics are not biocompatible and require certified hermetic encapsulation before the concept can be adapted for use in humans. As the optical sensor, in contrast to bioelectrical and biochemical sensors, does not need direct contact with the body, it can be mounted in a hermetic housing. For this purpose, a titanium

package with glass feedthroughs can be employed, similar to standard cardiac pacemakers but with a transparent sapphire window for the optical sensor.

For subcutaneous ECG measurements, flexible copper foils with a thickness of 20 μm and an electroplated gold layer on top were used as electrodes. For a final implantable version, these foils can be replaced by pure gold foils, to ensure biocompatibility. Before digitalization, the signal from the ECG electrodes was high-pass filtered with a cut-off frequency of 0.5 Hz, then differentially amplified by an instrumentation amplifier, and finally low-pass filtered at 150 Hz. This filtering ensures that only the frequency band containing the actual ECG is recorded with an improved signal-to-noise ratio.

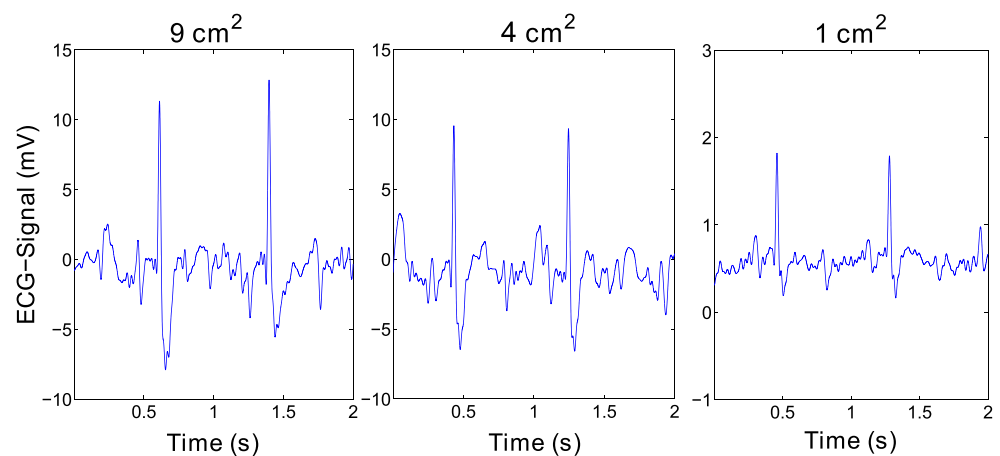
4 Results

4.1 Measurement description

The sensor described in Section 3 was tested and evaluated during two surgical interventions. In both cases, a sheep was used as subject. The animal experiments were approved by the local ethics committee and performed in compliance with the rules and regulations of the German animal protection law. Human care was provided in accordance with the 'Principles of Laboratory Animal Care', as formulated by the National Society for Laboratory Animal Medicine and the 'Guide for the Care and Use of Laboratory Animals' published by National Academy Press (NIH Publication No. 88-23).

Two female sheep (*Texel sheep hybrid*), each four years old, with body weights of 109 kg and 128 kg, were pre-medicated intramuscularly with midazolam (0.5 mg/kg) and ketamine (20 mg/kg), and anesthetized with propofol (2–4 mg/kg). Endotracheal intubation was followed by volume-controlled ventilation (12–14 breaths/min at 10–15 ml/kg tidal-volume, 5 mmHg positive end-expiratory

Fig. 5 ECG signals from electrodes of different size, at a spacing of 3 cm, acquired subcutaneously on a neck muscle



pressure) with setting adjustment to normalize oxygen and carbon dioxide concentrations and pH values. Anesthesia was maintained with isoflurane (1.0–1.5%), fentanyl (2–5 $\mu\text{g}/\text{kg}/\text{h}$) and ketamine (10 $\text{mg}/\text{kg}/\text{h}$), while fluid requirements were substituted with Ringer solution (5–10 $\text{ml}/\text{kg}/\text{h}$).

ECG, body-temperature and oxygen saturation were monitored continuously. A stomach tube was placed to avoid gastroesophageal reflux and a surgical incision was made in the neck for vascular access to the carotid artery. As a reference for the following measurements, the arterial blood pressure was acquired by a fluid-filled catheter in the carotid artery with connection to an extracorporeal transducer. In the second experiment, a tip-catheter (SPR-524I, Millar Instruments) was placed in the carotid artery, at a distance of approximately 20 cm from the PPG sensor. Data recording was performed by a 16 bit DAQ Card (National Instruments) with a sampling rate of 10 kHz. Further surgical neck incisions were made for placing subcutaneous ECG electrodes and PPG sensors.

Blood pressure variations were induced by intravenous injection of dopamine (0.05–0.1 mg/kg), which results in a quick rise followed by a slow decrease of the arterial blood pressure. To reach a stable plateau of arterial blood pressure, a continuous dopamine dose of 0.3–0.8 $\text{mg}/\text{kg}/\text{h}$ was supplied by a perfusor pump. In the first experiment, five quick dopamine sweeps were performed within four hours. In the second experiment, the pressure was varied by four dopamine boli and two perfusor pump sweeps within four hours. These variations will be discussed in the following sections. The corresponding pressure slopes are outlined later in Fig. 12.

4.2 Subcutaneous ECG

Flat, flexible gold-coated copper-electrodes of different size and with different spacings were used to compare the signal strengths of the ECG, detected subcutaneously, directly at the left and right sides of the neck muscle of the sheep.

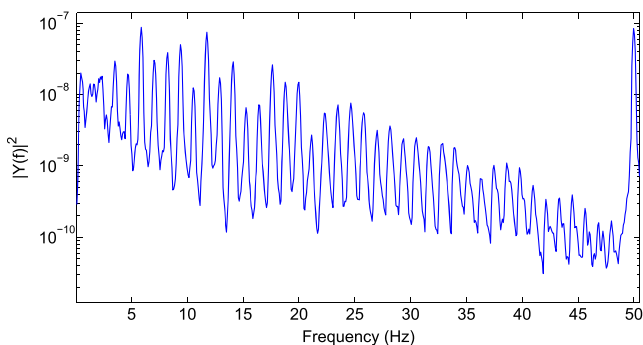


Fig. 6 Power spectral density of an ECG signal measured on subcutaneous tissue with 4 cm^2 electrodes at 3 cm spacing

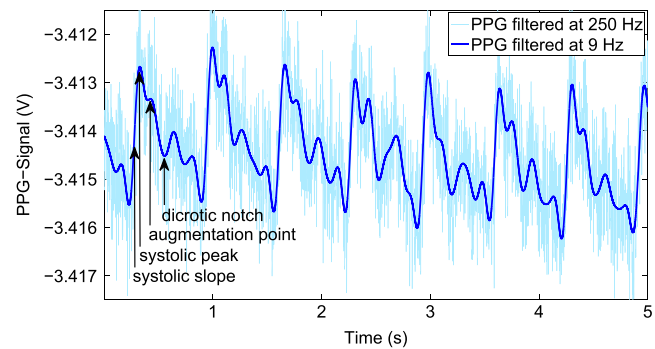


Fig. 7 Photoplethysmographic signal measured on subcutaneous muscle tissue, low-pass filtered at 9 Hz and at 250 Hz. The shape of the curve is similar to that of a PPG measured at a finger. The steep systolic rise and the reflections of the pressure wave are clearly visible

The amplitudes of the prominent R-peaks, as shown in Table 2, are low compared to the extracorporeally measured ECG amplitudes of 70 mV using adhesive electrodes with an active area of 9 mm^2 . Regardless of their size, the signal quality of all electrodes is sufficient for the determination of PTT. Figure 5 shows the measured results at a spacing between the two electrodes of 3 cm. The important and relevant QRS complex can be reliably detected. By analyzing the power spectral density of the ECG signal, overtones of up to 50 Hz become visible, as seen in Fig. 6. This measurement clearly indicates that even detailed information of the signal can be measured on subcutaneous tissue.

Increasing the spacing between the electrodes from 3 to 8 cm almost doubles the signal strength. In addition, the signal from electrodes of 4 cm^2 area is 20 times stronger than that of 1 cm^2 electrodes. Further increasing the area does not significantly enhance the amplitude. Only the smallest tested electrodes of 1 cm^2 area did not deliver a suitable ECG-signal when placed at the smallest spacing of 1 cm.

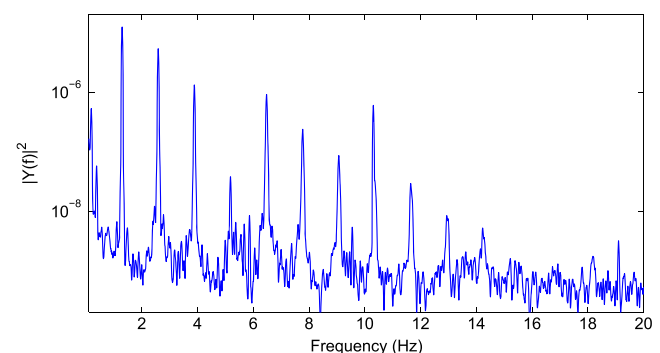
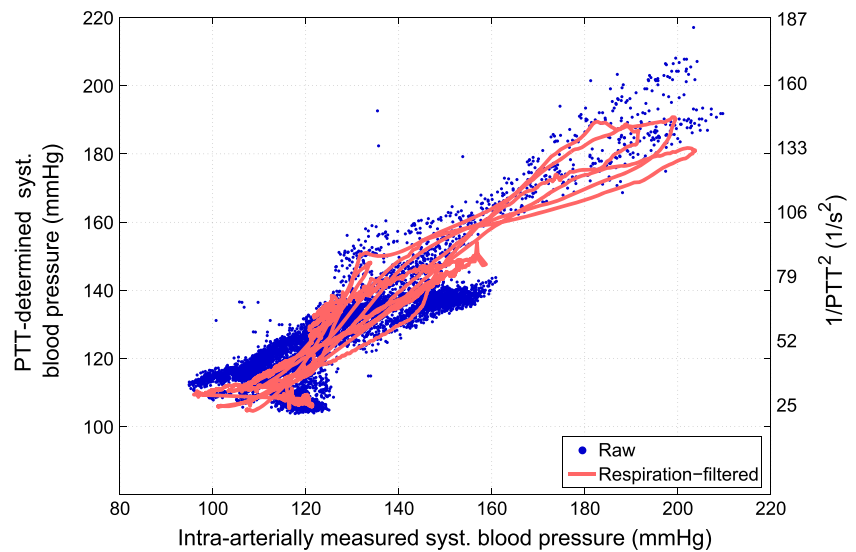


Fig. 8 Power spectral density of a subcutaneously recorded photoplethysmogram over 60 s; the heart frequency of 1.35 Hz and 10 overtones are well above the noise floor

Fig. 9 Blood pressure determined using subcutaneously acquired PTT vs. intra-arterially measured reference values. The *right y-axis* shows the calculated values in units of $1/s^2$. The *left y-axis* shows the values for the curve fit using Eq. 6. The *dotted data* represent the original raw data, whereas the *dashed curves* refer to respiration filtered data. The applied filter is a moving average over 20 pulses



4.3 Photoplethysmograms

For recording photoplethysmographic data subcutaneously, the sensors were positioned on the neck part of the musculus trapezius and nearby at the musculus cleido-occipitalis for subjects one and two, respectively. For both sensor locations, the pulse waves travel from the heart through the aortic arch, arteria subclavia and arteria cervicalis. From there, the pulses are passed to smaller arterioles, which deliver the blood to the muscles used for the measurement. The length of the arterial path between heart and sensor is approximately 40–50 cm.

It was seen that photoplethysmographic signals could be acquired on the neck muscles of both subjects. The amplitude of the detected pulsatile signal, which is shown in Fig. 7, is a factor of about 20 smaller than a standard reflective PPG signal measured on a human finger. The ratio between detected pulsatile and constant signal component is around 1:2000. This small value can be explained by the reduced capillary density of the neck muscle compared to that found under the skin of the fingers. The signal is subject

to power-line interference at multiples of 50 Hz; therefore low-pass filtering is necessary to extract the plethysmogram, as it is seen in the two plots of Fig. 7. Both the infrared as well as the red wavelength delivered excellent signal quality. As PTT determination requires only one wavelength, the following results employ the measured data from the infrared source.

To our knowledge, there is only one previous publication which shows subcutaneously measured PPG signals (Turcott and Pavek 2008), compared with which the measurement curves shown here have greater detail. All characteristic parts of the pulsatile signal, as known from signals measured by an extracorporeal pulse oximeter, are clearly visible: the steep systolic slope, a dominant peak followed by an augmentation caused by reflections in the blood vessels, a weaker diastolic decrease and the respiration dependent low-frequency oscillation of the PPGs. Figure 8 shows the power spectral density of the signal, where the heart frequency of 1.35 Hz and 10 overtones are adequately resolved.

As the measurements were performed under narcosis, no motion artifacts corrupted the signal. The implanted sensor is likely to be less sensitive to movement artifacts than a standard pulse oximeter, since the sensor is surgically attached to the tissue.

4.4 Pulse transit time

PTT was determined using the R-peak of the subcutaneous ECG signal and the maximum of the first derivative of the PPG signal, which represents the systolic slope. From measured PTT values, blood pressure follows by means of Eq. 6. As the constants in the equation are unknown, the values for $1/PTT^2$ were linearly fitted to the measured intra-arterial

Table 3 Comparison of different approaches for determination of systolic blood pressure, based on measurement of 12 000 pulses using two animal subjects without respiration filter. *r* is the Pearson’s correlation coefficient between the measured intra-arterial systolic reference pressure and the indirectly determined pressures

Method	r	Std. deviation	Mean abs. deviation
PTT, R-peak to systolic slope	0.89	9.8 mmHg	7.8 mmHg
PTT, R-peak to systolic peak	0.80	12.8 mmHg	9.0 mmHg
PPG amplitude	0.42	19.0 mmHg	14.5 mmHg

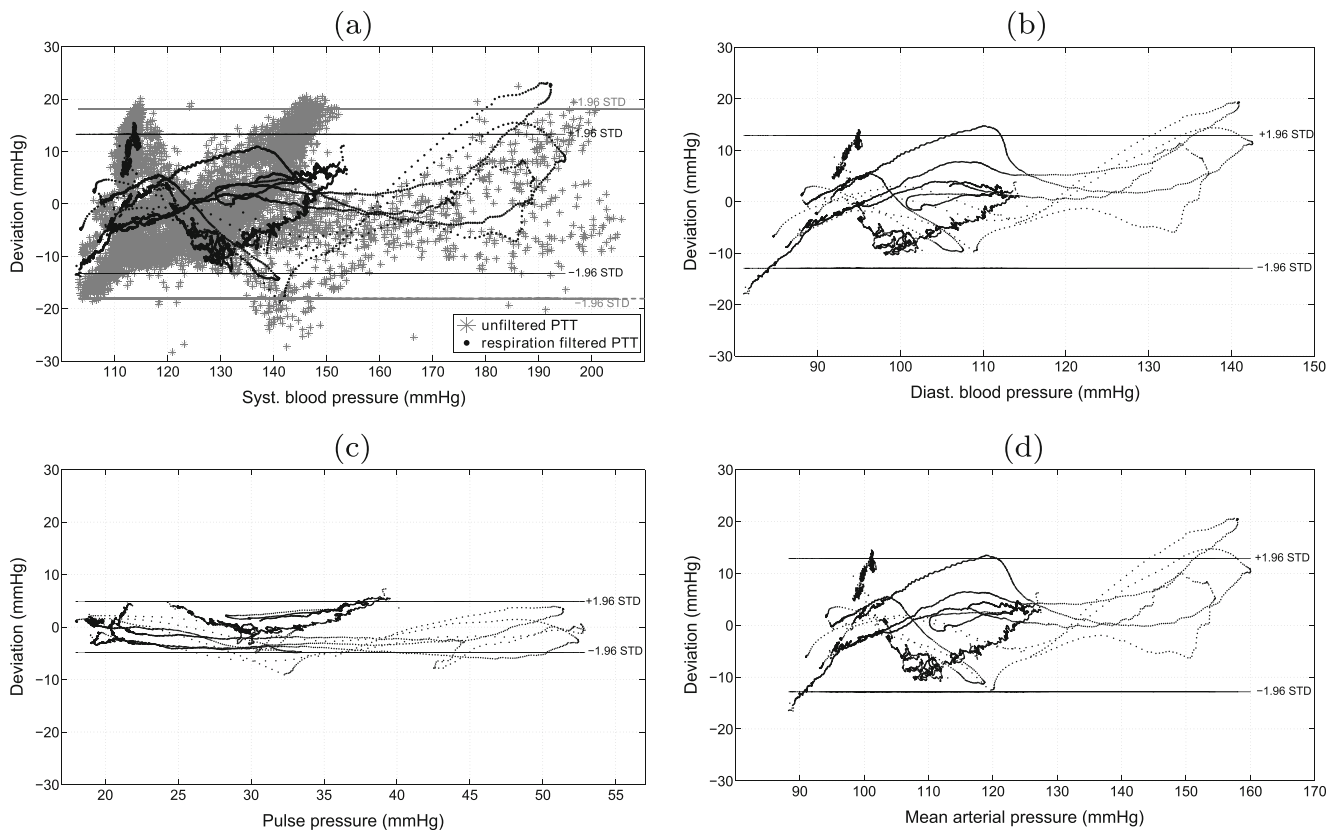


Fig. 10 Bland-Altman plots for different PTT-based pressure quantities. The *x-axis* shows the averaged values of reference and PTT-based pressure, the *y-axis* gives the corresponding deviation between these quantities for 8500 pulses from one subject. The deviations do not show any correlation with the blood pressure level, corroborating the PTT method and assumed linear model of Eq. 6. The *horizontal lines*

include 95 % of the data, given by ± 1.96 standard deviations (STD). **a** Systolic blood pressure. The gray points describe the raw measurement data; the black points represent the respiration filtered values over 20 pulses of the same dataset. **b** Respiration filtered data of diastolic blood pressure. **c** Respiration filtered data of arterial pulse pressure. **d** Respiration filtered data of mean arterial pressure

reference blood pressure to obtain values for the slope m and offset c .

Blood pressure as well as PTT vary with respiration. These variations have a phase difference which changes over time. Therefore, the effect of respiration has been filtered out in both the pressure signal and the PTT using a moving-average filter over 20 pulses. Figure 9 compares the systolic blood pressures from the reference measurement and as determined from PTT, with and without respiration filter. A slight hysteresis between the ascending

and descending blood pressure slopes is visible. For this case, PTT was determined using the systolic slope of the PPG-signal.

Table 3 compares the accuracy of two different PTT definitions, which use the R-peak of the ECG-signal as starting point. One approach takes the steepest part of the systolic slope as the reference point in the PPG for PTT measurement, the other one employs the systolic peak. The method using the maximum slope shows better correlation with the reference blood pressure value. The temporal

Table 4 Various blood pressure quantities determined by PTT from 12 000 pulses of two subjects. PTT is determined using the systolic slope as the reference point. The table is based on the same data set as Table 3, but filtered with respect to respiration effects

Method	R	Std. deviation	Mean abs. deviation
PTT-based systolic BP	0.94	6.7 mmHg (5.3 %)	5.5 mmHg (4.4 %)
PTT-based diastolic BP	0.85	6.5 mmHg (6.6 %)	5.3 mmHg (5.3 %)
PTT-based mean arterial pressure	0.89	6.4 mmHg (6.1 %)	5.3 mmHg (4.9 %)
PTT-based pulse pressure	0.95	2.4 mmHg (8.7 %)	1.9 mmHg (7.1 %)

Table 5 British Hypertension Society grading criteria for non-invasive blood pressure measurement devices

Grade	< 5 mmHg	< 10 mmHg	< 15 mmHg
A	60 %	85 %	95 %
B	50 %	75 %	90 %
C	40 %	65 %	85 %
D	worse	worse	worse

position of the diastolic minimum in the PPG signal, as another possible reference point, could not be detected reproducibly due to slight variations in the pulse shape.

As proposed by Turcott et al., the *amplitude* of the subcutaneous PPG signal can be used to estimate blood pressure as well (Turcott and Pavek 2008). Table 3 compares this method with the PTT-based approaches. The uncertainty is about two times higher for the amplitude estimation, probably due to variations in tissue perfusion, which makes this approach unsuitable for clinical implementation.

The differences between blood pressure values determined using PTT (with the systolic slope as the reference point) and those measured using a reference sensor over the full pressure range between 100 and 200 mmHg are shown in a Bland-Altman plot in Fig. 10a. Table 3 shows that the raw data has a mean deviation of 7.8 mmHg. Applying a filter to remove effects due to respiration improves this value to 5.5 mmHg (4.4 %).

Figure 10 and Table 4 show the precision for the PTT-determined systolic, diastolic, mean arterial and pulse pressure values, again using the systolic slope as the reference point. The same set of data as in Table 3 is used, but filtered to eliminate respiration effects. The high correlation coefficients suggest that PTT is a reliable means to determine the different pressure quantities. Figure 10 shows no increasing or decreasing trend with the pressure level and thus underscores the linear model from Eq. 6.

A calibration according to Table 1 with reference measurements at 120 and 170 mmHg would result in a mean accuracy error of 5.8 mmHg. The British Hypertension Society (BHS) has provided a grading system for devices measuring blood pressure (O’Brien et al. 1993) as shown in

Table 6 Sensor performance according to the British Hypertension Society criteria. The systolic blood pressure was measured by respiration filtered PTT

	< 5 mmHg	< 10 mmHg	< 15 mmHg
Subject 1	A: 65.1 %	A: 92.6 %	A: 96.7 %
Subject 2	B: 50.3 %	A: 85.6 %	A: 98.9 %
All	B: 54.8 %	A: 87.7 %	A: 98.3 %

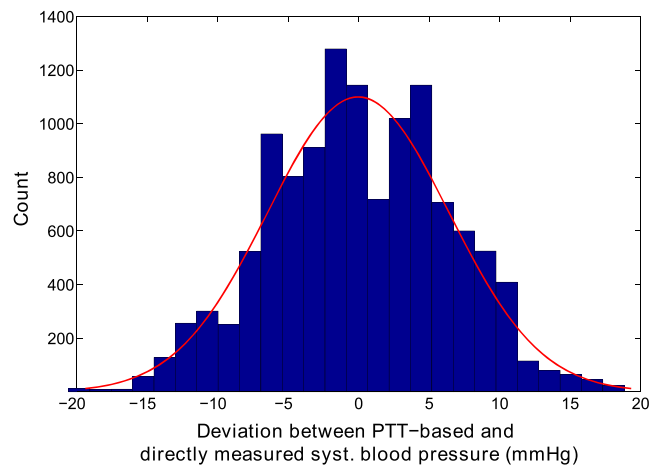


Fig. 11 Histogram of the deviations from the reference measurement for PTT-based systolic blood pressure for all 12 000 pulses of the measurements from subjects 1 and 2

Table 5. The blood pressure sensor performance, based on subcutaneously measured PTT values from 12 000 pulses measured on the two subjects, using these criteria is shown in Table 6. For criterion 1 (< 5 mmHg), the sensor is rated with 'B', for all other criteria, it fulfills the conditions for grade 'A'. As a result, the subcutaneous PTT-measurement is a grade 'B' blood pressure monitor.

The histogram in Fig. 11 summarizes the precision of the systolic blood pressure measurements for both *in vivo* experiments. More than 12 000 pairs of directly measured and PTT-derived blood pressure values were compared, showing a mean absolute deviation and a standard deviation of 5.5 and 6.7 mmHg, respectively.

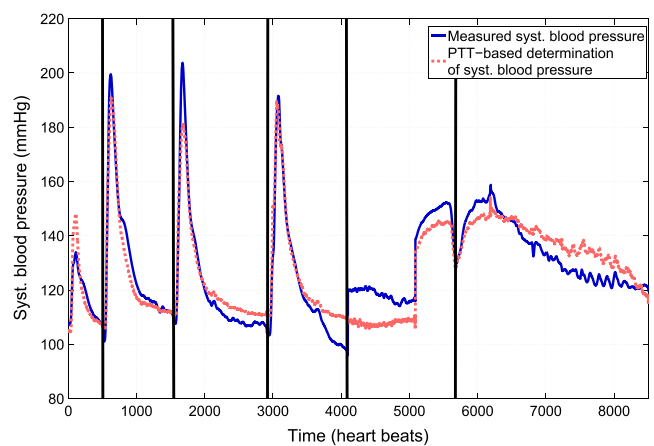


Fig. 12 Directly measured and PTT-determined blood pressure. The plot shows 6 sweeps; the delays between the sweeps have been removed. The first four variations were caused by injection of a dopamine bolus. For the final two slower variations, a perfusor was used to inject dopamine

Figure 12 displays the absolute values of directly measured (intra-arterial) and PTT-determined blood pressure for 6 different blood pressure sweeps. The first 4 sweeps were realized by bolus injections of dopamine, the last 2 variations by slow administration of dopamine with a perfusor. Even in the case of fast pressure variations, induced by the bolus, the optical approach precisely follows the measured intra-arterial pressure.

5 Conclusion

Photoplethysmographic signals acquired from subcutaneous muscle tissue open new prospects for continuously monitoring cardiovascular parameters by minimally invasive methods. Based on the good quality of the measured photoplethysmograms, pulse transit time could be determined when used in combination with subcutaneously placed flexible ECG-electrodes and a clear correlation between PTT and blood pressure was demonstrated. According to the BHS grading criteria, the device can be classified as a blood pressure sensor of grade 'B', with a mean deviation of 5.5 mmHg. This makes PTT a promising means for continuously monitoring blood pressure by an implantable but extravascular and cuff-less approach. Moreover, the quality of the PPG signals makes pulse contour analysis possible and, by extending the functionality of the sensor with a second light source, also allows the determination of blood oxygen saturation.

References

- S. Ahmad, S. Chen, K. Soueidan, I. Batkin, M. Bolic, H. Dajani, V. Groza, Electrocardiogram-assisted blood pressure estimation. *IEEE Trans. Biomed. Eng.* **59**, 608–618 (2012)
- H. Asada, P. Shaltis, A. Reisner, S. Rhee, R. Hutchinson, Mobile monitoring with wearable photoplethysmographic biosensors. *Eng. Med. Biol. Mag. IEEE* **22**(3), 28–40 (2003). doi:10.1109/MEMB.2003.1213624
- D. Bergel, The static elastic properties of the arterial wall. *J. Physiol.* **445**, 156–3 (1961)
- J. Blacher, R. Asmar, S. Djane, G. London, M. Safar, Aortic pulse wave velocity as a marker of cardiovascular risk in hypertensive patients. *Hypertens. - J. Am. Heart Assoc.* **33**, 1111–1117 (1999)
- C.P. Chua, C. Heneghan, in *Proceedings 28th Annual International Conference of the IEEE Engineering in Medicine and Biology Society EMBS '06*. Continuous blood pressure monitoring using eeg and finger photoplethysmogram, 5117–5120 (2006). doi:10.1109/IEMBS.2006.259612
- S. Deb, C. Nanda, D. Goswami, J. Mukhopadhyay, S. Chakrabarti, in *Proceedings International Conference on Convergence Information Technology*. Cuff-Less Estimation Of Blood Pressure Using Pulse Transit Time And Pre-Ejection Period, pp. 941–944 (2007). doi:10.1109/ICCIT.2007.4420381
- R. Farra, N. Sheppard, L. McCabe, R. Neer, J. Anderson, J. Santini, M. Cima, R. Langer, First-in-human testing of a wirelessly controlled drug delivery microchip. *Science Translational Medicine.* **4**(122), 122ra21 (2012)
- J. Fiala, P. Bingger, D. Ruh, K. Foerster, C. Heilmann, F. Beyersdorf, H. Zappe, A. Seifert, An implantable optical blood pressure sensor based on pulse transit time. *J. Biomed. Microdevices* (2012). doi:10.1007/s10544-012-9689-9
- P. Fung, G. Dumont, C. Ries, C. Mott, M. Ansermino, in *Proceedings 26th Annual International Conference of the Engineering in Medicine and Biology Society EMBC*. Continuous Noninvasive Blood Pressure Measurement By Pulse Transit Time. **1**, 738–741 (2004). doi:10.1109/IEMBS.2004.1403264
- Y.C. Fung, *Biomechanics: Circulation* (Springer, 2010)
- C. Lee, C. Lee, Y. Zhang, in *Proceedings IEEE EMBS Asian-Pacific Conference on Biomedical Engineering*, ed. by Y. Zhang. Cuffless and Noninvasive Estimation Of Blood Pressure Based On A Wavelet Transform Approach, 148–149 (2003). doi:10.1109/APBME.2003.1302627
- S.C. Millasseau, J.M. Rittera, K. Takazawab, P.J. Chowienyca, Contour analysis of the photoplethysmographic pulse measured at the finger. *J. Hypertens.* **24**, 1449–1456 (2006)
- J. Moyle, *Pulse Oximetry*, 2nd edn. BMJ (2002)
- E. Nye, The effect of blood pressure alteration on the pulse wave velocity. *Br. Heart J.* **26**, 261–265 (1964)
- E. O'Brien, J. Petrie, W. Littler, M. de Swiet, P. Padfield, D. Altman, M. Bland, A. Coats, N. Altkins, The british hypertension society protocol for the evaluation of blood pressure measuring devices. *J. Hypertens.* **11**, 43–62 (1993)
- E. O'Brien, R. Asmar, L. Beilin, Y. Imai, J.M. Mallion, G. Mancia, T. Mengden, M. Meyers, P. Padfield, P. Platini, G. Parati, T. Pickering, J. Redon, J. Staessen, G. Stergiou, P. Verdecchia, European society of hypertension recommendations for conventional, ambulatory and home blood pressure measurement. *J. Hypertens.* **21**, 821–848 (2003)
- S. Richard, J.M.R. Irwin, *Manual of Intensive Care Medicine* (Williams & Wilkins, 2009)
- T. Stieglitz, S. Kammer, K. Koch, S. Wien, A. Robitzki, in *7th Conference of the International Functional Electrical Stimulation Society (IFESS)*. Encapsulation of flexible biomedical microimplants with parylene c (2002)
- R. Turcott, T. Pavek, Hemodynamic sensing using subcutaneous photoplethysmography. *Am. J. Physiol. - Heart and Circ. Physiol.* **295-6**, 2560–2572 (2008)
- S.I.B.F. Wilkinson, I.M. Jansen, J.C. Spratt, G.D. Murray, J.R. Cockcroft, D. Webb, Reproducibility of pulse wave velocity and augmentation index measured by pulse wave analysis. *J. Hypertens.* **16**, 2079–2084 (1998)